Available online at www.sciencedirect.com
ScienceDirect
Trans. Nonferrous Met. Soc. China 30(2020) 2590−2598
Transactions of Nonferrous Metals Society of China
www.tnmsc.cn

Effect of rapid cold stamping on fracture behavior of long strip *S′* phase in Al−Cu−Mg alloy

Cai-he FAN[1,2], Ling OU[1,2], Ze-yi HU[1], Shu WANG[3], Jun-hong WANG[3]

1. College of Metallurgy and Material Engineering, Hunan University of Technology, Zhuzhou 412007, China;
2. Anhui Jianye Science and Technology Co., Ltd., Huaibei 235000, China;
3. 208 Research Institute of China Ordnance Industries, Beijing 102202, China

Received 6 January 2020; accepted 16 July 2020

Abstract: High-angle annular dark-field scanning transmission electron microscopy and selected area electron diffraction techniques were used to study the mechanism that underlies the influence of rapid cold-stamping deformation on the fracture behavior of the elongated nanoprecipitated phase in extruded Al−Cu−Mg alloy. Results show that the interface between the long strip-shaped *S′* phase and the aluminum matrix in the extruded Al−Cu−Mg alloy is flat and breaks during rapid cold-stamping deformation. The breaking mechanisms are distortion and brittle failure, redissolution, and necking. The breakage of the long strip *S′* phase increases the contact surface between the *S′* phase and the aluminum matrix and improves the interfacial distortion energy. This effect accounts for the higher free energy of the *S′* phase than that of the matrix and creates conditions for the redissolution of solute atoms back into the aluminum matrix. The brittle *S′* phase produces a resolved step during rapid cold-stamping deformation. This step further accelerates the diffusion of solute atoms and promotes the redissolution of the *S′* phase. Thus, the *S′* phase necks and separates, and the long strip-shaped *S′* phase in the extruded Al−Cu−Mg alloy is broken into a short and thin *S′* phase.

Key words: Al−Cu−Mg alloy; rapid cold stamping; nanoprecipitate; fracture behavior; breaking mechanism

1 Introduction

A heterogeneous microstructure that consists of hardened precipitates and dispersoids is the primary strengthening source of Al−Cu−Mg alloys [1,2]. The *S′* phase is a key strengthening precipitate in high-strength Al−Cu−Mg alloys and exhibits an orthorhombic structure with space group CMCM [3−6]. Strong plastic deformation can improve the precipitation phase characteristics, such as the morphology, size, distribution, and orientation relationship with the matrix, of aluminum alloy, improve its microstructure, and obtain microscale or even nanoscale fine-grained structures [6−11]. STYLES et al [12] studied the relationship between the resolution sequence of a supersaturated solid solution and the formation phase of the equilibrium *S* phase in Al−Cu−Mg alloy. The formation time of the *S* phase at high temperature is considerably shorter than that at low temperature. YANG et al [13] studied the effects of applied stress on the aging kinetics and precipitated phase morphology of Al−Cu−Mg alloy and found that applied stress promotes the precipitation of the *S′* phase by changing the force contrast between the *S′* phase and the *θ′* phase in competitive precipitation. NOURBAKHSH and NUTTING [14] found that the flaky *θ′* phase is severely bent and broken after the large reduction cold-rolling of A1−4%Cu alloy. MURAYAMA et al [15] observed a needle-like *θ′* transition phase in the equal-

Foundation item: Project (19A131) supported by Key Scientific Research Project of Hunan Province, China; Project (2019JJ60050) supported by the Natural Science Foundation of Hunan Province, China
Corresponding author: Ling OU; Tel: +86-731-22183432; E-mail: ouling24@126.com
DOI: 10.1016/S1003-6326(20)65404-8

diameter extrusion deformation of A1−Cu alloy, which gradually decomposed into short-chain particles during several equal-angle extrusion processes until it redissolved into the matrix. HUANG et al [16] used cold rolling to change the dislocation cell structure in Al−Cu−Mg alloy with a low Cu/Mg mass ratio and obtained a high-density dispersed fine S'' phase. ZHAO et al [17] found that the S phase continuously converts to the Ω phase with an increase in cold deformation degree in the cold rolling deformation of 2024 aluminum alloy. ZHANG et al [18,19] studied the effect of multidirectional compressive deformation on the precipitation phase of Al−Cu alloy and found that the precipitation sequence of the supersaturated solid solution formed by the redissolution of the precipitates under strong plastic deformation is related to heating temperature, deformation, and postdeformation grain size.

It can be seen that the existing literature is mainly to study the characteristics of the precipitated phase and the re-dissolution phenomenon under the conditions of conventional plastic deformation. There is still a lack of rapid cold punching as the method of plastic deformation, and the impact of the nano-precipitated phase on the microstructure of the alloy is discussed. In order to study the mechanism that underlies the influence of rapid cold-stamping deformation on the fracture behavior of the elongated nanoprecipitated phase in extruded Al−Cu−Mg alloy, this experiment is based on the rapid solidification of fine-grained Al−Cu−Mg alloy billet prepared via spray forming. The fracture behavior of the long strip S' phase in Al−Cu−Mg alloy during rapid cold stamping is also studied. The analysis of the breaking mechanism of the S' phase lays a theoretical foundation for the systematic study of the evolutionary law and strengthening mechanism of the long-shaped S' phase.

2 Experimental

A rapidly solidified fine-grained Al–Cu–Mg alloy cylindrical ingot was prepared on a self-developed SD380 large-scale injection molding apparatus. Table 1 provides the chemical composition of the alloy. The cylindrical ingot was extruded into a d30 mm round bar on a 1250 T extruder at 450 °C with an extrusion ratio of 15:1. The round bar was cut into a small cylinder with dimensions of d30 mm × 20 mm and rapidly cold-stamped for four passes at 25 °C. The sketch maps of rapid cold stamping are presented in Fig. 1. The small cylindrical sample was first placed in the mold, and the first small punch was used to rapidly cold-stamp along the center of the sample to complete the first pass of rapid cold forming. Then, a large-diameter punch was used for cold-stamping along the first pass forming hole, and four passes of rapid cold-stamping were completed in sequence. The parameters of rapid cold stamping are listed in Table 2.

Table 1 Composition of alloy studied (wt.%)

Cu	Mg	Mn	Si	Fe	Al
3.91	1.63	0.38	<0.03	<0.03	Bal.

The samples for microstructure observation were obtained from the center wall of the cylinder fabricated through rapid cold forming. The morphology, size, and distribution of the nanoprecipitated phase of the sample were analyzed through JEM-F200 transmission electron

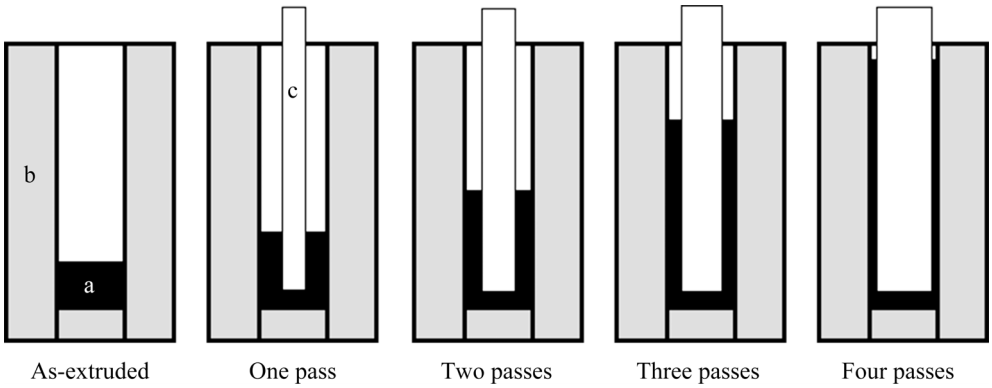

Fig. 1 Sketch maps of rapid cold punching (a—Sample; b—Drawing die; c—Punch)

Table 2 Technological parameters of rapid cold punching

Pass number	Diameter/mm	Velocity/(mm·s^{-1})
One	10	30
Two	14	25
Three	20	20
Four	27	15

microscopy (TEM). The transmission samples were mechanically prethinned to approximately 80 μm and then subjected to twin-jet electropolishing. The electrolytes were nitric acid and methanol (volume ratio of 1:3) at a temperature of less than −25 °C. The electron microscopy parameters of the high-angle annular dark-field scanning transmission electron microscope (HAADF–STEM) were as follows: acceleration voltage of 200 keV, electron beam half convergence angle of 10 mrad, and beam spot diameter of 0.20 nm.

3 Results

3.1 As-extruded sample

Figure 2 shows a HAADF−STEM images of the as-extruded Al−Cu−Mg alloy. The elongated S' phase in the as-extruded alloy is regularly distributed in the aluminum matrix; the lengthwise dimension of the elongated S' phase is less than 300 nm, and a number of dislocations are distributed around the precipitated phases (Fig. 2(a)). Figure 2(b) shows the interface between the elongated S' phase and the aluminum matrix observed along the $[001]_{Al}$ direction. The shape of the S' phase is regular, and the interface with the aluminum matrix along the length direction of the S' phase is flat.

3.2 Rapid cold punching sample

Figure 3 depicts a HAADF−STEM image of the extruded Al−Cu−Mg alloy after two passes of rapid cold-stamping deformation. The number of S' phases increases drastically, and the S' phases are irregularly distributed in the aluminum matrix. The length of the S' phase after two passes of rapid cold-stamping deformation is the same as that of the extruded sample (Fig. 3(a)). The morphology of most S' phases has changed, and the interface between the S' phase and the aluminum matrix is not flat. The S' phase distorts and breaks during rapid cold-stamping deformation (Fig. 3(b)). The high-magnification field TEM image shows that the long S' phase is broken, the broken interface is visible, and one S' phase is broken into several parts (*A*, *B*, *C*, and *D*). Each part undergoes drastic twisting, *B* is rotated by the α_1 angle with respect to *A*, *C* is rotated by the α_2 angle with respect to *B*, and *D* is rotated by the α_3 angle with respect to *C* (Fig. 3(c)).

Figure 4 shows a HAADF–STEM image of the extruded Al–Cu–Mg alloy after three passes of rapid cold-stamping deformation. As shown in the figure, the number of S' phases in the alloy is reduced significantly compared with those in the specimens after two passes of rapid cold-stamping deformation. However, a large number of short rod-shaped S' phases are observed, and the S' phases

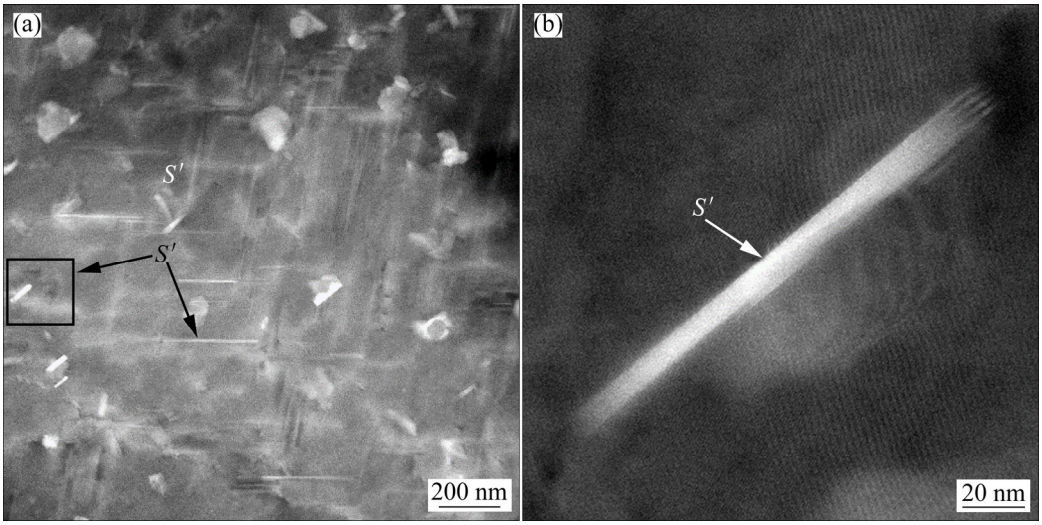

Fig. 2 HAADF−STEM images of S' precipitates in as-extruded Al−Cu−Mg alloy viewed along $[001]_{Al}$ direction

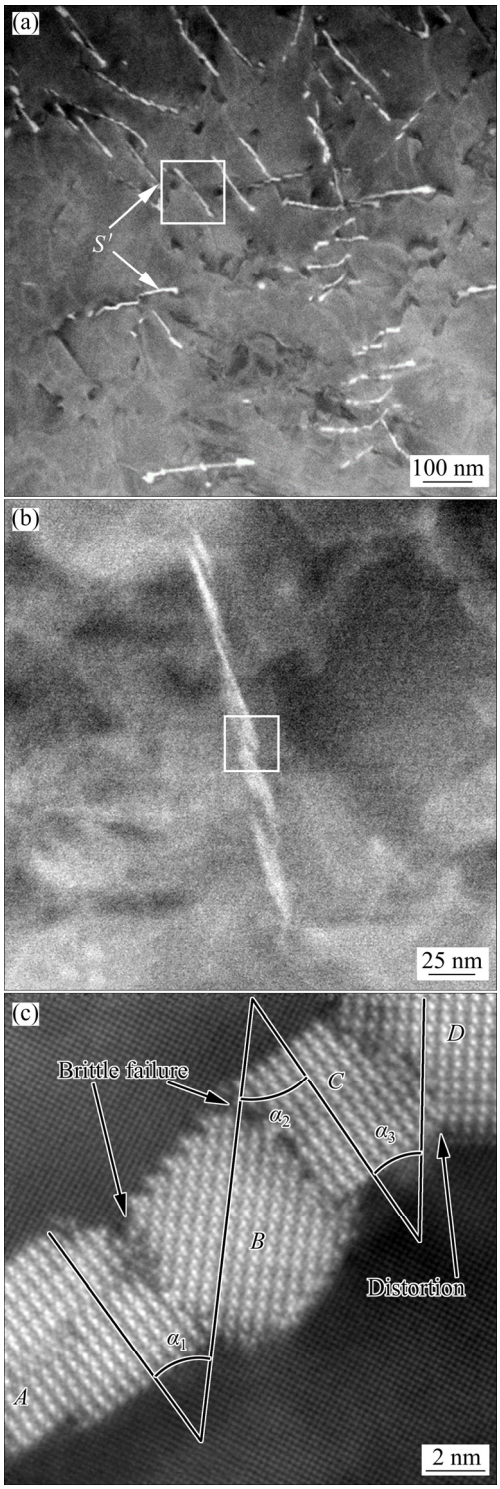

Fig. 3 HAADF−STEM images of S' precipitates in Al−Cu−Mg alloy undergoing two passes viewed along $[001]_{Al}$ direction

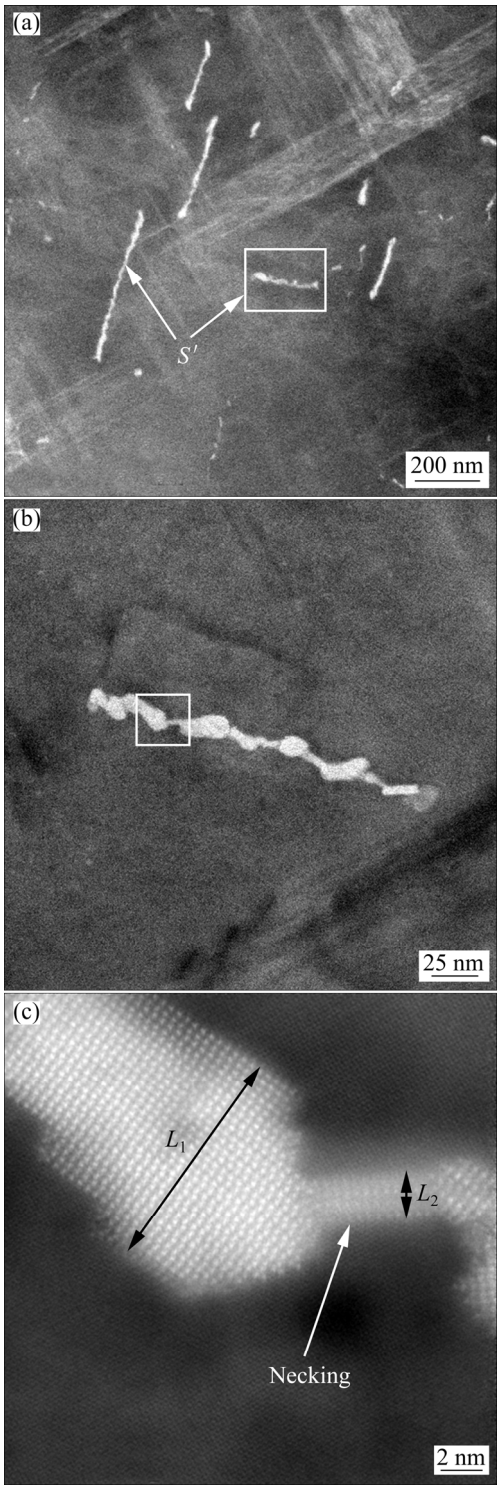

Fig. 4 HAADF−STEM images of S' precipitates in Al−Cu−Mg alloy undergoing three passes viewed along $[001]_{Al}$ direction

remain irregularly distributed in the aluminum matrix (Fig. 4(a)). As the degree of the deformation increases, the morphology of the S' phase changes, the degree of distortion is aggravated, and the broken part of the S' phase begins to separate from the base metal (Fig. 4(b)). The high-magnification TEM image shows that the region of the long strip-shaped S' phase is necked, and L_1 is considerably larger than L_2. The ends of necked region tend to separate as the value of L_1/L_2 increases (Fig. 4(c)).

Figure 5 shows a HAADF−STEM image of the extruded Al−Cu−Mg alloy after four passes of rapid cold-stamping deformation. This figure shows that the number of S' phases in this sample has increased compared with those in the sample after three passes of rapid cold-stamping deformation.

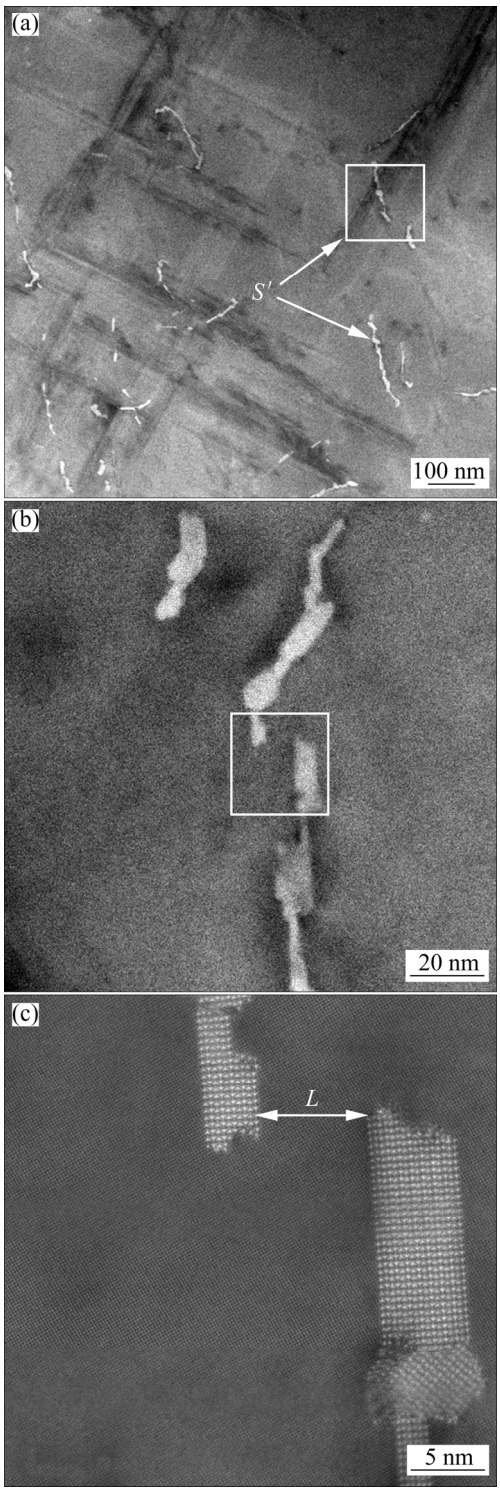

Fig. 5 HAADF−STEM images of S' precipitates in Al−Cu−Mg alloy undergoing four passes viewed along $[001]_{Al}$ direction

The S' phase is short and thin, and remains irregularly distributed in the aluminum matrix (Fig. 5(a)). After four passes of rapid cold-stamping deformation, the long strip-shaped S' phases in the extruded sample are nearly broken into short rods, resulting in a considerable reduction in the size of the S' phase in the aluminum matrix (Fig. 5(b)). The high-magnification field TEM image shows that the necked component of the long strip-shaped S' phase has disappeared. The ends of the necked region have separated, and the distance between the two parts is L. The S' phase has broken into several independent parts (Fig. 5(c)).

4 Analysis and discussion

4.1 Breaking mechanism of nano-precipitated phase during rapid cold stamping

In this experiment, rapid cold stamping deformation has three major characteristics: low deformation temperature (25 °C), large strain, and high strain rate. In accordance with the general criteria of PUGH and related research, the Al_2CuMg phase is a typical brittle phase [20,21]. Therefore, combined with the results of this experiment, the breaking mechanisms of the long strip-shaped S' phase in the extruded Al−Cu−Mg alloy induced by rapid cold-stamping deformation are as follows.

(1) Distortion and brittle fracture

The long strip-shaped S' phase acts as the major strengthening phase of the extruded Al−Cu−Mg alloy and is regularly distributed in the aluminum matrix, and the S' phase is flat with the aluminum matrix (Fig. 2). During rapid cold stamping deformation, the soft aluminum matrix is subject to severe shear deformation, which causes the hard S' phase to distort under the strong shear deformation force. The torsion angle between parts C and D is α_3. When the deformation force reaches a certain level, i.e., when the torsion angle reaches a certain value (e.g. α_1 or α_2), brittle S' phase fractures and interfaces are formed between A and B or B and C (Fig. 3(c)). With the distortion and brittle fracture of the long strip-shaped S' phase, the drastic increase in brittle interfaces considerably increases the contact surface between the precipitated phase and the aluminum matrix. The interfacial distortion energy between the precipitated phase and the aluminum matrix is improved, and diffusion conditions for the solute atoms are created. The

redissolution of the S' phase during rapid cold-stamping deformation accelerates. The distortion and brittle fracture model of the long strip-shaped S' phase is shown in Fig. 6.

(2) Resolving and necking

Figure 7 presents a HAADF–STEM image showing the resolved step of the S' phase and a model of redissolution and necking in the sample subjected to three passes of rapid cold stamping. The resolved step is clearly observable in the S' phase, and the arrows in the figure are the resolving direction. The resolved step is the product of the twisting and brittle fracture of the S' phase during strong plastic deformation. Given that the distortion and breakage of the long S' phase considerably improve the interfacial distortion energy between the S' phase and the aluminum matrix, the solute atoms located at the region of the S' phase with high distortion energy are highly likely to be redissolved. The local accelerated redissolution of the S' phase results in a significant reduction in the size of the S' phase in this region, i.e., the formation of a neck (Fig. 4(c)), which further increases the interfacial distortion between the precipitated phase and the aluminum matrix and can accelerate redissolution at the necked position. Necking disappears when the value of L_1/L_2 is infinite, and the disappearance of the neck causes the separation of the two parts of the precipitated phase (Fig. 5(c)).

The presence of high numbers of resolved steps in the S' phase is associated with the large contact surface of the broken particles within the aluminum matrix. The diffusion of solute atoms is facilitated. In accordance with the classical thermodynamic view [22], a certain equilibrium vacancy concentration in the crystal exists at any

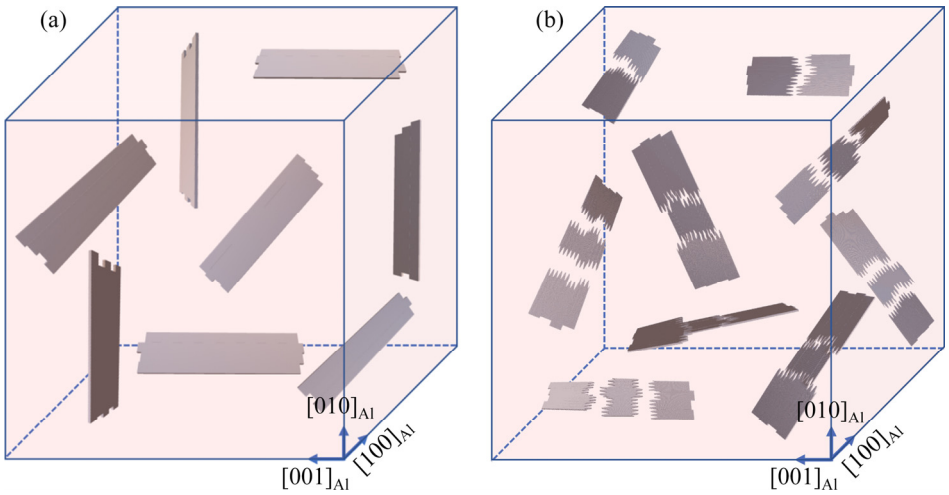

Fig. 6 Distortion and brittle fracture model of long strip-shaped S' phase: (a) As-extruded; (b) Two-pass

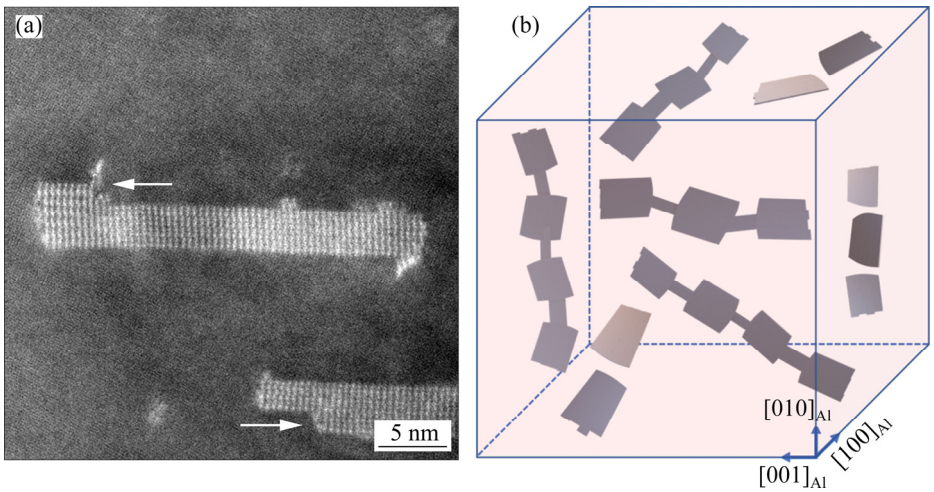

Fig. 7 HAADF−STEM image (a) and necking model (b) of precipitated phase in Al−Cu−Mg alloy undergoing three passes

temperature and changes positions continuously. The existence and movement of vacancies create conditions for atomic diffusion. The dislocation density increases significantly during rapid cold deformation. Dislocations will generate a large number of vacancies in the matrix during delivery and movement, and each time, a rapid cold shear deformation will produce a large number of new vacancies. Simultaneously, the long strip-shaped S' phase is constantly twisted and broken during rapid cold-stamping deformation, and the contact interfaces between S' phase and aluminum matrix increase and are accompanied by a large number of vacancies. The number of vacancies undergoing strong deformation increases sharply [19,23], the diffusion rate of solute atoms can be increased by five orders of magnitude, and volume diffusion can be increased by eight orders of magnitude. The alloy was prepared through spray-forming rapid solidification technology and had fine grains and uniform structure. The average grain size was approximately 5 μm. During rapid cold-stamping deformation, the grains are further refined into nanoscale, and thus, the grain boundary area increases. It also provides an atomic diffusion channel for the redissolution of the precipitated phase, and this channel considerably promotes the redissolution of the precipitated phase.

4.2 Fracture mechanism of nano-precipitated phase during rapid cold stamping

Under the condition of rapid cold-stamping deformation, the long strip-shaped S' phase in the extruded Al−Cu−Mg alloy undergoes intense distortion, brittle fracture, redissolution, necking, and separation (Figs. 3−5). Consequently, the long strips of S' phases transform into short rods or even redissolve and disappear. In contrast with that of the extruded sample, the brittle fracture of the long strip S' phase remarkably increases the contact surface of the S' phase and the matrix, and interface distortion can be drastically improved. This phenomenon results in the free energy of the S' phase being higher than that of the matrix. The disturbance of the energy balance between the reprecipitated phase and the matrix creates conditions for the redissolution of the solute atoms into the matrix. The binding energy (E_{coh}) and the formation enthalpy of ΔH [20,21] between the Al_2Cu and Al_2CuMg phases are calculated using the first principle equations:

$$E_{coh} = E_{total}^{AB} - [x_A E_{atom}^{A} + (1 - x_A) E_{atom}^{B}] \quad (1)$$

$$\Delta H = E_{total}^{AB} - [x_A E_{solid}^{A} + (1 - x_A) E_{solid}^{B}] \quad (2)$$

where E_{total}^{AB} is the average energy per atom of each intermetallic compound; E_{atom}^{A} and E_{atom}^{B} are the energy of free atoms A and B, respectively; E_{solid}^{A} and E_{solid}^{B} are the average energy per atom in stable elemental A and B, respectively; x_A represents the mole fraction of atom A in the compound.

VASILS et al [24] believed that two types of processes will occur when precipitates are completely dissolved into the matrix. The first process is lattice transformation, wherein the lattice of the precipitated phase changes into the matrix lattice. The second process is the diffusion of the redissolved solute atoms in the matrix; this phenomenon increases the uniformity of the supersaturated solid solution. The results show that the S' phase in the as-extruded alloy redissolves into the aluminum matrix after three passes of rapid cold-stamping deformation and becomes refined. The rapid cold-stamping deformation temperature of the alloy in this test is low, and if solute atoms uniformly disperse into the matrix by diffusion to redissolve the precipitate phase, the redissolution rate must be extremely slow.

In accordance with the solid-state phase transition theory [22], the critical size of the nucleus (r_c) is expressed as follows:

$$r_c = f\left(\frac{\sigma}{\Delta G} - U\right) \quad (3)$$

where σ is the surface free enthalpy, ΔG is the difference in volume free enthalpy between the parent phase and the precipitated phase, and U is the strain energy produced by the two phases. With the fragmentation of the precipitated phase, σ, ΔG, and U change significantly, resulting in an increase in the critical size (r_c) of the precipitated phase. The redissolution amount and rate of the precipitated phase increase.

In summary, the redissolution of nano-precipitates during strong plastic deformation plays an important role in structural evolution. The distortion and brittle fracture of the S' phase during rapid cold-stamping deformation results in a resolved step, which accelerates the redissolution of

the S' phase. The partial redissolution of the phase promotes the further necking of the S' phase and results in the separation of various parts of the S' phase, resulting in the fragmentation of the elongated S' phase in the extruded alloy and its transformation into a short and thin S' phase.

5 Conclusions

(1) The interface between the strip-shaped S' phase and the aluminum matrix in the extruded Al−Cu−Mg alloy is flat and breaks during rapid cold-stamping deformation. The fracture mechanisms are distortion, brittle fracture, redissolution, and necking.

(2) The brittle fracture of the long S' phase increases the contact surface between the S' phase and the aluminum matrix, improves the interfacial distortion energy, and accounts for the higher free energy of the S' phase than that of the matrix. The disturbance of the energy balance between the S' phase and the matrix creates diffusion conditions for the redissolution of the solute atoms into the matrix.

(3) The redissolution of nanoprecipitates during strong plastic deformation plays an important role in structural evolution. The break of the local S' phase accelerates its redissolution, resulting in the fragmentation of long S' phase into short and thin S' phase.

References

[1] CHENG S, ZHAO Y H, ZHU Y T, MA E. Optimizing the strength and ductility of fine structured 2024Al alloy by nano-precipitation [J]. Acta Mater, 2007, 55(17): 5822−5832.

[2] WANG Jian-qiu, ZHANG Bo, WU Bo, MA Xiu-liang. Size-dependent role of *S* phase in pitting initiation of 2024 Al alloy [J]. Corrosion Science, 2016, 105(2): 183−189.

[3] WANG S C, STARINK M J. Two types of *S* phase precipitates in Al−Cu−Mg alloys [J]. Acta Materialia, 2007, 55(3): 933−941.

[4] LIU Zi-ran, CHEN Jiang-hua, WANG Shuang-bao, YUAN Ding-wang, YIN Mei-jie, WU Cui-lan. The structure and the properties of *S*-phase in AlCuMg alloys [J]. Acta Materialia, 2011, 59(19): 7396−7405.

[5] KILAAS R, RADMILOVIC V. Structure determination and structure refinement of Al_2CuMg precipitates by quantitative high-resolution electron microscopy [J]. Ultramicroscopy, 2001, 88(1): 63−72.

[6] WANG Jian-qiu, ZHANG Bo, ZHOU Yang-tao, MA Xiu-liang. Multiple twins of a decagonal approximant embedded in *S*-Al_2CuMg phase resulting in pitting initiation of 2024Al alloy [J]. Acta Materialia, 2015, 82(1): 22−31.

[7] KANG S B, LIM C Y, KIM H W, MAO J F. Microstructure evolution and hardening behavior of 2024 aluminum alloy processed by the severe plastic deformation [J]. Materials Science Forum, 2002, 396−402(2):1163−1168.

[8] YANG Bing, MA Xiu-liang. Local decomposition induced by dislocations inside θ' precipitates in Al−Cu alloy [J]. Journal of Chinese Electron Microscopy Society, 2013, 32(4): 289−294. (in Chinese)

[9] WANG Shuang-bao, CHEN Jiang-hua, YIN Mei-jie, LIU Zi-ran, YUAN Ding-wang. Double atomic wall based dynamic precipitates of the early-stage *S*-phase in AlCuMg alloys[J]. Acta Materialia, 2012, 60(19): 6573−6580.

[10] AN Li-hui, CAI Yang, LIU Wei, YUAN Shi-jian, ZHU Shi-qiang, MENG Fan-cheng. Effect of pre-deformation on microstructure and mechanical properties of 2219 aluminum alloy sheet by thermomechanical treatment [J]. Transactions of Nonferrous Metals Society of China, 2012, 22(2): 370−375.

[11] YIN Mei-jie, CHEN Jiang-hua, WANG Shuang-bao, LIU Zi-ran, CHA Li-mei. Anisotropic and temperature-dependent growth mechanism of *S*-phase precipitates in Al−Cu−Mg alloy in relation with GPB zones [J]. Transactions of Nonferrous Metals Society of China, 2016, 26(1): 1−11.

[12] STYLES M J, MARCEAU R K W, BASTOW T J, BRAND H E A, GIBSON M A, HUTCHINSON C R. The competition between metastable and equilibrium *S*(Al_2CuMg) phase during the decomposition of Al−Cu−Mg alloys [J]. Acta Materialia, 2015, 98(1): 64−80.

[13] YANG Pei-yong, ZHENG Zi-qiao, XU Fu-shun, LI Shi-chen, LI Jian, ZHOU Ming. Effect of external stress on kinetics of precipitation and morphologies of precipitates in Al−Cu−Mg alloy with high Cu/Mg ratio [J]. Chinese Journal of Rare Metals, 2006, 30(3): 324−328. (in Chinese)

[14] NOURBAKHSH S, NUTTING J. The high strain deformation of an aluminium−4%copper alloy in the supersaturated and aged conditions [J]. Acta Metallurgica, 1980, 28(3): 357−365.

[15] MURAYAMA M, HORITA Z, HONO K. Microstructure of two-phase Al−1.7at%Cu alloy deformed by equal-channel angular pressing [J]. Acta Mater, 2001, 49(1): 2l−29.

[16] HUANG Yu-jin, CHEN Zhi-guo, ZHENG Zhi-qiao. A conventional thermo-mechanical process of Al−Cu−Mg alloy for increasing ductility while maintaining high strength [J]. Scripta Materialia, 2011, 64(5): 382−385.

[17] ZHAO Yun-long, YANG Zhi-qing, ZHANG Zhen-jun, SU Guo-yue, MA Xiu-liang. Double-peak age strengthening of cold-worked 2024 aluminum alloy[J]. Acta Materialia, 2013, 61(5): 1624−1638.

[18] ZHANG Zi-zhao, XU Xiao-chang, HU Nan, QU Xiao, CHEN Zhen-xiang. Re-ageing behavior of Al−Cu alloy after re-dissolution of precipitated phases caused by severe plastic deformation[J]. Journal of Central South University (Science and Technology), 2010, 41(5): 1782−1790. (in Chinese)

[19] ZHANG Zi-zhao, XU Xiao-chang, LIU Zhi-yi, XIA Qing-kun, ZENG Su-min. Re-precipitate behavior of supersaturated solid solution of Al−Cu alloy caused by severe plastic deformation during subsequent deformation [J]. The Chinese Journal of Nonferrous Metals, 2009, 19(11):

1962−1968. (in Chinese)
[20] PUGH S F. Relations between the elastic moduli and the plastic properties of polycrystalline pure metals [J]. Philosophical Magazine, 1954, 45(367): 823−843.
[21] ZHANG Jian, HUANG Ya-ni, MAO Cong. Structural, elastic and electronic properties of $\theta(Al_2Cu)$ and $S(Al_2CuMg)$ strengthening precipitates in Al−Cu−Mg series alloys: First-principles calculations [J]. Solid State Communications, 2012, 152(23): 2100−2104.
[22] LIAO Fei, FAN Shi-tong, DENG Yun-lai, ZHANG Jin. First-principle calculations of mechanical properties of Al_2Cu, Al_2CuMg and $MgZn_2$ intermetallics in high strength Aluminum alloys [J]. Journal of Aeronautical Materials, 2016, 36(6): 1−8. (in Chinese)
[23] YU Yong-ling. Principles of metallography [M]. 2nd ed. Beijing: Metallurgical Industry Press, 2013. (in Chinese)
[24] VASILS L S, LONMAEV I L, ELSUKOV E P. On the analysis of the mechanisms of the strain-induced dissolution of phases in metals [J]. Physics of Metals and Metallography, 2006, 102(2): 186−197.

快速冷冲对 Al−Cu−Mg 合金长片状 *S′*相破断行为的影响

范才河[1,2]，欧 玲[1,2]，胡泽艺[1]，王 舒[3]，王俊红[3]

1. 湖南工业大学 冶金与材料工程学院，株洲 412007；
2. 安徽建业科技有限公司，淮北 235000；
3. 中国兵器工业第二〇八研究所，北京 102202

摘 要：采用高角度环形暗场(HAADF)扫描透射电子显微镜(STEM)和选区电子衍射(SAED)技术，研究快速冷冲强变形对挤压态 Al−Cu−Mg 合金长片状纳米析出相破断行为的影响机理。实验结果表明：挤压态 Al−Cu−Mg 合金中长片状 *S′*相与铝基体界面平整，在快速冷冲强变形过程中发生明显破断，其破断机制主要为扭曲、脆断、回溶和缩颈。长片状 *S′*相的破断，增加了 *S′*相与铝基体的接触面，提高了界面畸变能，从而导致 *S′*相的自由能高于基体自由能，为溶质原子回溶至铝基体的扩散创造条件。脆性 *S′*相在快速冷冲强变形过程中产生“回溶台阶”，进一步加速溶质原子的扩散，促进 *S′*相的回溶，造成 *S′*相缩颈而导致各部分的分离，从而使挤压态长片状 *S′*相“碎化”成短而细的 *S′*相。

关键词：Al−Cu−Mg 合金；快速冷冲；纳米析出相；破断行为；破断机制

(Edited by Xiang-qun LI)